



## **Preliminary Analysis of Air Ingress Experiment QUENCH-16 using RELAP/SCDAPSim3.5 and MELCOR 1.8.6**

**Leticia Fernandez-Moguel**

Paul Scherrer Institute

CH-5230, Villigen PSI, Switzerland

Leticia.fernandez-moguel@psi.ch

### **ABSTRACT**

Post-test analyses for the air ingress experiment QUENCH-16 were performed by PSI. The calculations were performed with a local version of RELAP5/SCDAPSim3.5 and MELCOR1.8.6\_YR. Both codes represent air oxidation; nevertheless the modelling treatment is different. The pre-oxidation and air phase were consistent and in fair agreement with both codes. There is no evidence from the measured temperatures/O<sub>2</sub> starvation that breakaway occurred during the experiment, this was further supported by the analysis. A strong oxidation excursion took place during the reflood. This feature of the experiment was not expected from pre-test predictions. The excursion may have been triggered by breakaway, nitride reaction and/or an alpha-layer formation during O<sub>2</sub> starvation. It remains an open question and suggests that further improvement in the modelling is needed.

### **1 INTRODUCTION**

In recent years air ingress scenarios have drawn attention due to the possibility of accelerated fuel rod degradation during a severe accident and the consequent release of some fission products, most notably ruthenium [1, 2]. Furthermore, the recent accident at Fukushima Daiichi drew attention to the possibility of an air ingress scenario in the Spent Fuel Pond. Several experiments have been performed to study the effect on air ingress on fuel bundles under early phase severe accident conditions: CODEX-AIT1 and AIT2 [3] which looked at air ingress with lightly pre-oxidised rods in a small electrically heated-bundle, the larger QUENCH-10 experiment [4] which investigated the effect of air ingress on fuel rods heavily pre-oxidised in steam using PWR materials and configuration, PARAMETER-SF4 [5] which was very similar to QUENCH-10 transient but with materials and configuration prototypical of VVER reactors and the recent separate-effect test on zirconium cladding degradation [6] which has shown that nitrogen-containing atmospheres lead to strong degradation of the cladding material.

The recent air ingress experiment QUENCH-16 was successfully performed at Karlsruhe Institute of Technology (KIT) on 27<sup>th</sup> July 2011. The experiment was performed within the EU part-sponsored LACOMEKO programme [7, 8], and was proposed and partnered by the Hungarian Institute, AEKI [9]. The aim of the experiment was to extend the existing database on the transient behaviour during air ingress on a dried out and partially oxidised bundle. QUENCH-16 was complementary to the previous QUENCH-10 experiment. The main differences were in the preoxidation period before air ingress phase and the duration of oxygen starvation. QUENCH-10 was extensively preoxidized and included a short starvation period, whereas QUENCH-16 had a milder preoxidation and a longer starvation period. A primary test objective was to provide a prolonged period of oxygen starvation in order to study the reaction between partially oxidised cladding and nitrogen, in particular



- I. The bundle was heated by power increase to about 1450K; this marked the start of the pre-oxidation phase.
- II. The power was controlled to maintain more or less constant temperatures until the desired cladding oxidation was obtained. This was measured by the total H<sub>2</sub> generation.
- III. The power was reduced until 990K was reached. One corner rod was extracted in order to measure the oxide thickness.
- IV. The steam flow was replaced by air flow and the Ar flow was reduced. At the end of this phase the second corner rod was removed.
- V. Bottom water injection was initiated when the 1883K were observed

Table 1 summarises the main boundary conditions for Q-16 for each phase as well as the main times and temperatures. It is noted that the actual and nominal conditions were not identical. In particular there was a small but unquantified and unplanned flow of steam during the air phase.

Table 1: Main experimental phases

Phase		QUENCH-16 nominal	QUENCH-16 actual
I	T <sub>max,steam</sub> power increase to duration steam + argon flowrate	≈1450 K, ≈ 10 kW 1 h 15 min 3 + 3 g/s	≈1450 K, 10-11.5 kW 1 h 15 min 3.3 + 3 g/s
II	Pre-oxidation of the test bundle for at constant temperature of power: steam + argon flowrate	≈ 30 min 1430K, 11.5 kW, 3 + 3 g/s	≈ 30 min 1430K, 11.5 kW, 3.3 + 3 g/s
III	Intermediate cooling from to duration: power: steam + argon flowrate	≈ 1430 K ≈ 990 K 17 min 4 kW 3 + 3 g/s	≈ 1430 K ≈ 990 K 17 min 4 kW 3.3 + 3 g/s
IV	Air ingress and slow heat-up from to duration: oxygen starvation for power: steam flowrate: argon + air flowrate:	≈ 1000 K ≈ 1823 K ≈ 60 min ≈ 15 min 4 kW 0.0 g/s 1.0 + 0.2 g/s	990 K 1883 K 67 min 13 min 4 kW unquantified 1.0 + 0.2 g/s
V	Quenching of bundle at water flowrate:	≈ 11000 s 50 g/s	11341 s 50 g/s

### 3 MODELLING TOOLS

#### 3.1 RELAP5/SCDAPSim/Mod 3.5

The new RELAP5/SCDAPSIM/Mod 3.5 (SSim3.5) code was previously used in analyses of the PARAMETER SF4 experiment [14]. This code version recognises oxygen as an active species and nitrogen as a catalyst. The kinetic model takes as input the concentrations of oxygen, steam and nitrogen, along with the current local oxidation status of the cladding to determine the kinetics. A choice of different sets of parabolic oxidation correlations for steam or air is provided. In the present study Cathcart-Pawel [15]/Urbanic-Heidrick [16] (CP-UH) (CP at  $T < 1853$  K, UH at  $T > 1873$  K), was used for oxidation in steam and the default PSI model for air which uses the Uetsuka-Hofmann [17] kinetics for lower temperatures ( $T < 1623$  K) and CP-UH for higher temperatures ( $T > 1623$  K) in conjunction with the breakaway model in air. The PSI air oxidation model development and its physical basis were described in detail in [13].

A similar input model was used as in previous analyses of QUENCH [18, 19]. The input model comprised a single hydraulic channel for the test train including the lower and the upper volumes. Specifications of the flow channel and the rod surface areas were defined in the input and were determined from the dimensions of all the test section components, and was independent of the geometric arrangement (rectangular or hexagonal). The water cooling systems for the central and upper bundle sections were also modelled with an external thermal boundary condition applied. Twenty axial nodes were used for the test train and the shroud, of which ten were for the 1024 mm heated tungsten section, four/one nodes represented the molybdenum and copper electrodes below the tungsten section, and similarly above it. The structures within the bundle were represented by five SCDAP components arranged in five concentric rings: the central unheated rod (ring 1), the eight inner heated rods (ring 2), the twelve outer heated rods (ring 3), the four corner rods (ring 4) and the shroud-insulation-jacket assembly (ring 5). Radiation heat transfer between all the components was modelled by SCDAP according to their respective temperatures. All of the SCDAP components were radially subdivided with sufficient resolution to resolve the temperature distribution through the various material layers. The insulation spans only the central bundle which was reflected in the model by varying the composition along the axial length. The Stainless Steel outer cooling jacket was modelled as a set of RELAP5 heat structures in contact with the cooling system on the inside while the laboratory temperature was specified as the external boundary condition. The noding of the hydraulic volumes, junctions and boundary condition, and the SCDAP components is shown in Figure 3 (left). The boundary conditions (power, flows, and timings of the main phases) were defined to follow as closely as possible the experimental values.

#### 3.2 Melcor 1.8.6\_YR

The MELCOR code version 1.8.6\_YR (M186\_YR) [12] was used for the analysis. This code version allows to model oxidation in air, but does not include any model for breakaway. The steam and air oxidation kinetics are treated as parabolic. The MELCOR default correlation for steam oxidation is UH in both temperature ranges, but in order to be consistent with the SSim3.5 version, the CP/UH correlation was used in M186\_YR for both steam and air phase by means of a sensitivity card.

The input model used as in previous analyses of OECD ISP-45 on QUENCH-06 [20] was refined as it is shown in figure 3 (right), thus more resolution was needed to model the fast oxygen consumption and thus resolve the oxygen starvation front. The bundle was

divided into twenty-two axial levels and four rings. The innermost ring contained the single unheated fuel rod simulator, the second ring contained eight heated rod simulators, and the third ring contained twelve heated rod simulators and four corner rods. The outermost ring contained the shroud. Thirty-two volumes were used to represent the core; sixteen corresponded to the inner part of the bundle where ten of the volumes lied within the heated region between 0 mm and 1024 mm; another sixteen volumes represented the annular region between the shroud and the cooling jacket (gray). The cooling systems were represented as a fixed temperature boundary. Additional volumes were used to represent the lower and upper plenum, the water-filled sinks at the extremes of the bundle (green), and the isolated region between the top of the bundle outlet plenum and the upper heat sink (blue). The heater rods are represented as shown in figure 3.

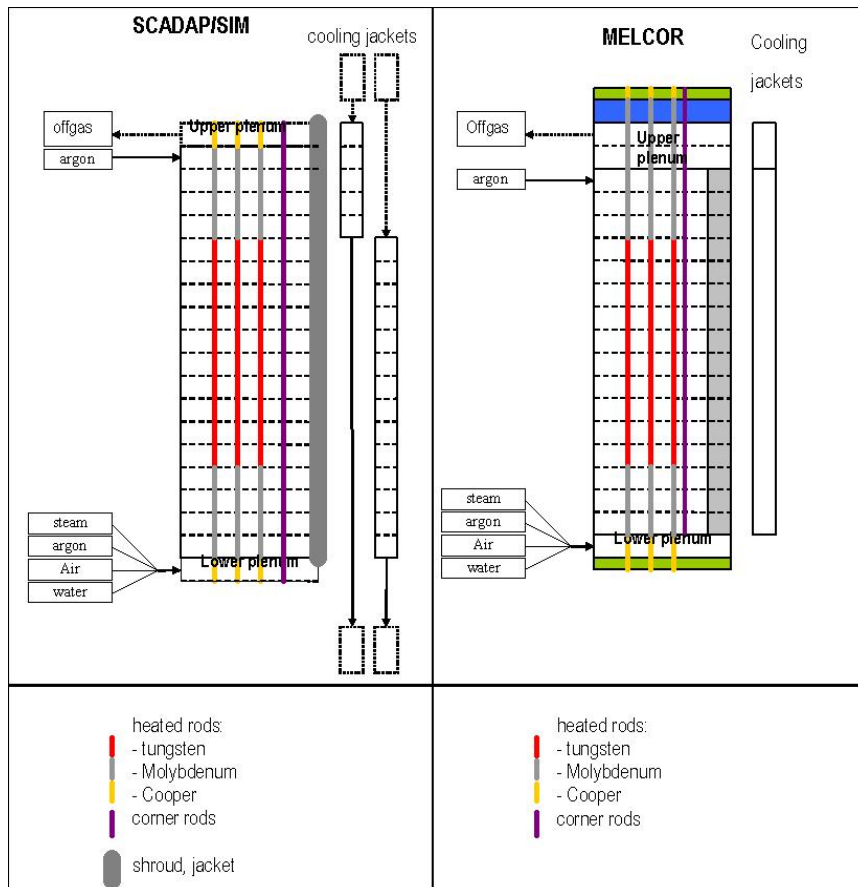


Figure 3: Nodalization: (left) SCDAP/SIM and (right) MELCOR

## 4 ANALYSIS OF QUENCH-16 WITH MELCOR AND RELAP5/SCDAP/SIM

### 4.1 Steam phase

Phases I, II, III (from table 1) were analysed together as the “steam phase”. In order to obtain the closest oxidation profile at the end of the steam phase, the external resistance was adjusted in the input for both codes. For SSim3.5 the best agreement was obtained with an external resistance of 3.8 m $\Omega$ , whereas for M186\_YR the best agreement was obtained with an external resistance of 3.6 m $\Omega$ . Both values were within the experimental estimated range. Figures 4 and 5 show the temperature profile and the hydrogen generation respectively. One can see that the maximum temperature (at the 950 elevation) was very similar with both codes. Nevertheless, the axial profile was slightly better predicted with M186\_YR. Both codes were very close in the prediction of the total hydrogen generation. The oxidation

thickness predicted at 950mm elevation in the corner rod was 180  $\mu\text{m}$  for SSIm3.5 and 166  $\mu\text{m}$  for M186\_YR the experimental measured value at the same location was 133  $\mu\text{m}$ .

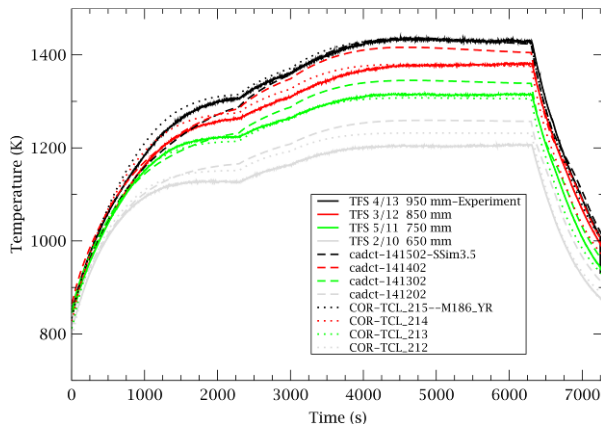


Figure 4: Temperature profile during the steam phase

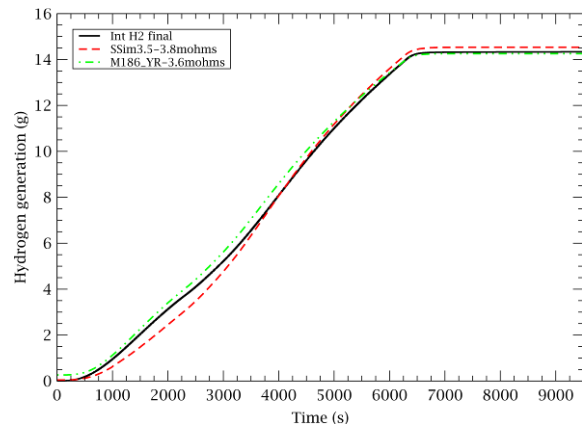


Figure 5: H2 production during the steam phase

## 4.2 Air phase

During phase IV, the influence of additional steam on the thermal response, oxygen consumption, and the possible breakaway was considered.

### 4.2.1 Extra source of steam

The switch from steam + argon to low flow of air + argon reduced the convective heat transfer and resulted in a temperature increase without at first any oxidation heat.

Figure 6 shows the unplanned source of steam that was observed at the offgas line. Three calculations were made using SSIm3.5: the first assuming that the steam observed in the offgas line was flowing through the bundle, the second where the steam was turned off at the beginning of starvation and the third which did not consider the extra source of steam. Separately in this way we compare the roles of steam as coolant and oxidant. Breakaway was disabled for these three calculations. One calculation was made with M186\_YR which included the source of steam.

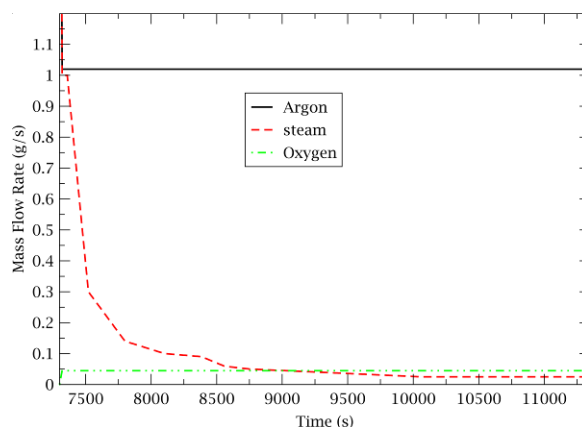


Figure 6: Extra source of steam during the air phase

Figure 7 shows the temperature at 650 mm elevation (This elevation was one of the hottest at the end of the air phase) and figure 8 shows the oxygen consumption. The increase in slope marks then onset of rapid oxidation. The calculations without additional steam resulted in earlier heat up and oxygen starvation. The calculations made with M186\_YR predicted an earlier heat up resulting in earlier oxygen starvation. The calculations where the

steam was included using SSIm3.5 was the one closer to the experimental values. The extra steam acted as a coolant as long as there is still oxygen available at the corresponding location (including after starvation onset). The calculations where the steam was turned off at the onset of oxygen starvation resulted in a lower maximum temperature. This shows that after oxygen starvation the steam was reacting and providing extra heat. This result is qualitatively consistent with the hydrogen measurement in the offgas line.

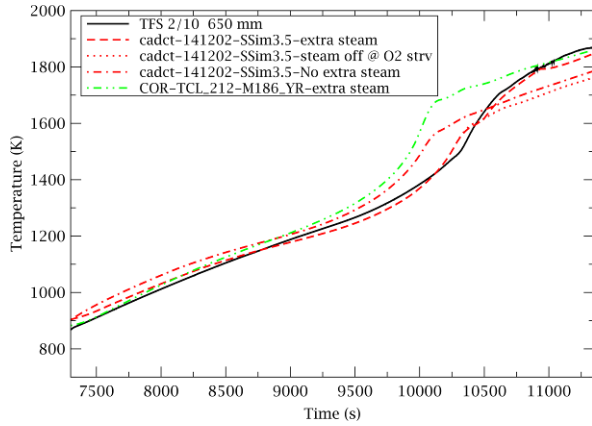


Figure 7: Temperatures at 650 mm elevation

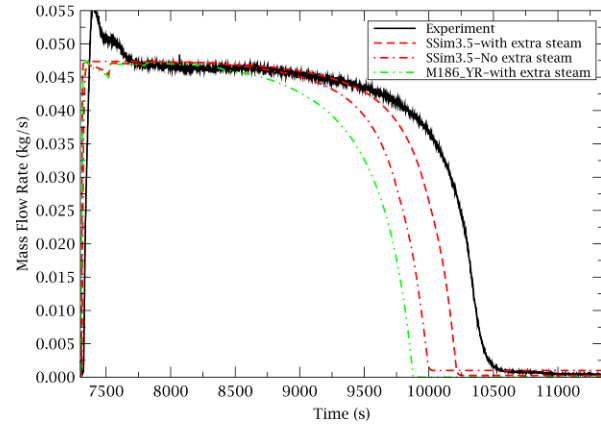


Figure 8: Oxygen consumption

Although the extra steam source was not planned it was fortuitous in that steam-air mixtures are believed to be more typical than air alone. It also allowed to verify that the codes can deal with both steam and air together. Both codes assume that the steam does not react as long as there is oxygen available. Figure 9 shows the  $H_2$  production, both codes overpredicted it; it is possible that not all the steam was consumed in the experiment. Another possibility is that not all the steam observed in the offgas measurement was flowing through the bundle. The steam source was considered in the following calculations.

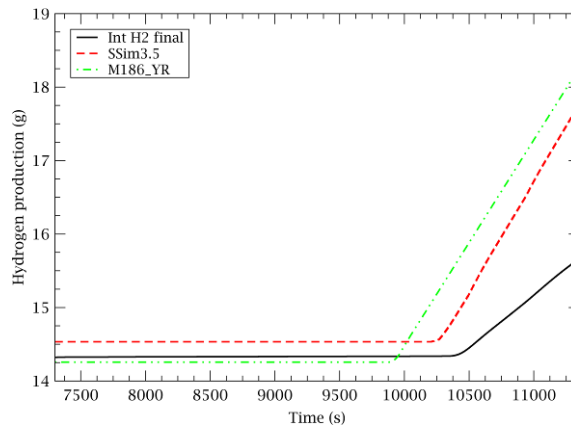


Figure 9:  $H_2$  generation during the air phase

#### 4.2.2 Breakaway

Breakaway was only evaluated with the SSIm3.5 code version, since M186\_YR does not have a breakaway model. Two cases were considered with the assumption of steam flow: Breakaway calculation was enabled (Bkwy) and breakaway calculation was disabled (No bkwy). Figures 10 and 11 show the axial temperature profile for the lower and upper elevation respectively. Figure 12 shows the oxygen consumption with and without breakaway. The temperatures increase and the oxygen starvation was reached faster than in the experiment when breakaway was calculated.

The best agreement was obtained when no breakaway was calculated. In fact the absence of any measured sudden increase in oxygen consumption or cladding temperature supported the view that no breakaway occurred during the experiment during the air phase. However breakaway was observed in the previous Q-10 experiment and it had been expected in Q-16. It is unclear why breakaway did not occur in this case. One possibility is that the very low oxygen concentration during Q-16 changes the oxidation kinetics. The effect of oxygen concentration on the kinetics has been previously observed in separate effect tests [21].

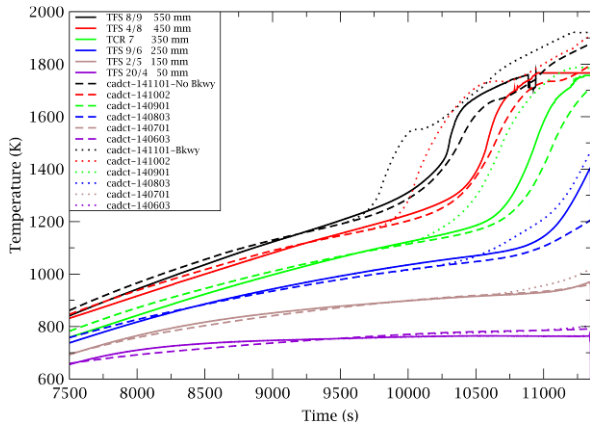


Figure 10: Temperatures for the lower elevations

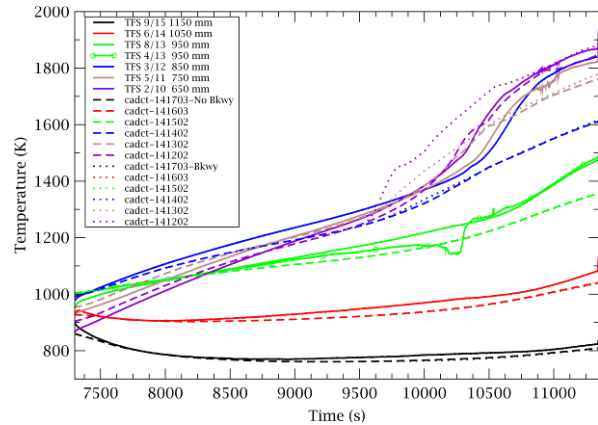


Figure 11: Temperatures for the higher elevations

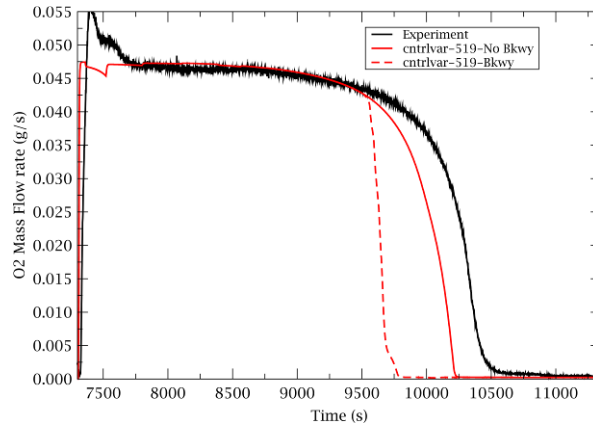


Figure 12: Oxygen starvation with and without breakaway

### 4.3 Reflood

Although no excursion was predicted by any of the codes during the pre-test analysis [10], unexpectedly high temperatures were observed during reflood. Neither of the codes reproduced it as it is shown in figure 13. SSim3.5 predicted no excursion and M186\_YR calculated a mild excursion, possibly due to the slightly higher temperatures at the beginning of the reflood. Furthermore, neither of the codes calculated anywhere near to the total hydrogen production observed during reflood (figure 14).

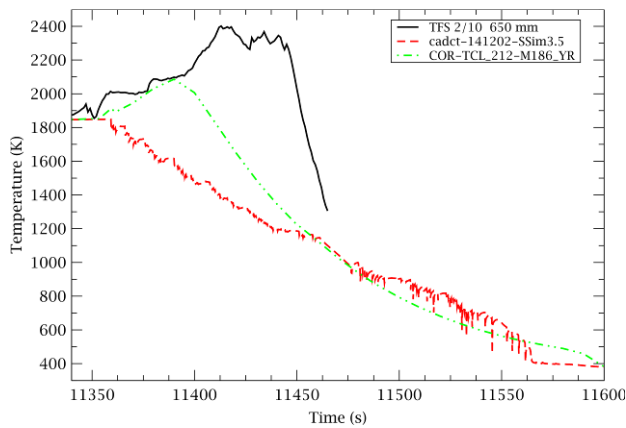
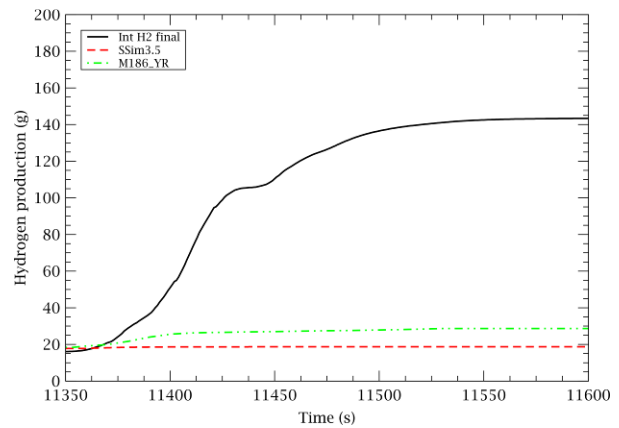


Figure 13: Temperatures during reflow

Figure 14: H<sub>2</sub> production during reflow

The causes of the excursion are not yet fully understood. However, one or more of the following process may have led to a possible mechanism for triggering the strong oxidation excursion during reflow: ZrN formation, reoxidation of the ZrN and nitrogen release during reflow, dissolution of the oxide into an  $\alpha$ -Zr(O) region.

- The experiment showed evidence of nitrogen uptake (about 29g). The formation of nitrides during the starvation period was confirmed by examination after the experiment. It is possible that the nitrides weakened the oxide layer and the thermal stresses during reflow promoted breakaway. Neither MELCOR nor SCDAP are able to predict a nitride reaction.
- There was evidence of nitrogen release (about 24g) during the reflow. This lasted for about 200s. During this time the reaction:  $\text{ZrN} + 2\text{H}_2\text{O} = \text{ZrO}_2 + 1/2\text{N}_2 + 2\text{H}_2$  would take place. The heat of reaction for it is  $\Delta H^\circ -252.8 \text{ kJ/mol(Zr)}$ . This would correspond to  $\sim 2.15 \text{ kW}$  of oxidation heat over a period of about 200 s and  $\sim 7\text{g}$  of H<sub>2</sub>. The amount of hydrogen that would correspond to this reaction is nowhere near to the experimental value.
- An oxygen stabilized  $\alpha$ -Zr (O) region may have been formed by diffusion of oxygen from the oxide layer into the underlying metallic layer during the long period of oxygen starvation. That would have reduced the oxide layer to  $\alpha$ -Zr(O) and hence drastically increased its susceptibility to oxidise and also to react with nitrogen. Experience in separate-effect tests has shown that the oxygen stabilized  $\alpha$ -Zr(O) layer reaction with nitrogen plays an important role during oxidation [22]. The codes are not able to model the  $\alpha$ -layer formation.

It is clear that these processes would have been connected during QUENCH-16 and it is not possible to separate their respective roles without further study involving complementary experimentation.

## 5 CONCLUSIONS

QUENCH-16 provided new data on air ingress scenarios. The main differences from the previous QUENCH air ingress experiment were the lower pre-oxidation and the low air flow which enabled the long period of oxygen starvation to be achieved. The fortuitous presence of air and steam together was more representative of a real situation.

The QUENCH-16 results were analysed with both MELCOR1.8.6\_YR and RELAP5/SCDAPSim3.5. The results were consistent with both versions and only slight differences were observed during the pre-oxidation phase, with both codes in fair agreement with the temperatures, hydrogen production and oxide thickness layer. The extra source of steam was evaluated. It was shown that the steam acted as a coolant as long as there was steam available and additional oxidant during oxygen starvation. Both codes were able to handle steam and air together.

MELCOR predicted earlier the temperature escalation which caused earlier oxygen starvation and slightly higher temperatures at the end of the air phase.

The calculation with no breakaway showed very good agreement with the temperatures and the oxygen starvation. The calculation with breakaway predicted too fast O<sub>2</sub> consumption and faster temperature escalation. Although it was expected, there are no indications that breakaway occurred during the experiment. One possible explanation is that the low oxygen concentration during the experiment may have influenced the kinetics.

The large excursion observed during reflood was not reproduced by either code. A previously damaged bundle, nitride reaction and  $\alpha$ -layer or a combination of all may be the cause of the excursion. It remains as an open question indicating a need for further improvement in the modelling, supported by suitable experimentation.

## **ACKNOWLEDGMENTS**

The author wishes to acknowledge the financial support of the Swiss Federal Nuclear Safety Authority, ENSI, and invaluable technical input from KIT (Germany).

## REFERENCES

- [1] F. C. Iglesias, C. E. L. Hunt, F. Garisto, and D. S. Cox, “Measured release kinetics of ruthenium from uranium oxides in air, proc. of int. seminar on fission product transport processes during reactor accidents”, Editor J. T. Rogers, Hemisphere Publishing Corp, Washington DC, 1990.
- [2] A. Auvinen, G. Brilliant, N. Davidovich, R. Dickson, G. Ducros, Y. Dutheillet, P. Giordano, M. Kunstar, T. Kärkelä, M. Mladin, Y. Pontillon, C. Séropian and N. Vér, “Progress on ruthenium release and transport under air ingress conditions”, Nucl. Eng. Des., 238, 2008, pp. 3418–3428.
- [3] I. Shepherd et al., Oxidation Phenomena in Severe Accidents (OPSA)—Final Report. INV-OPSA (99)-P008, EUR 19528 EN, 2000.
- [4] G. Schanz, M. Heck, Z. Hozer, L. Matus, I. Nagy, L. Sepold, U. Stegmaier, M. Steinbrück, H. Steiner, J. Stuckert, P. Windberg: “Results of the QUENCH-10 experiment on air ingress”. Wissenschaftliche Berichte, FZKA-7087, SAM-LACOMERA-D09, Karlsruhe, May 2006.
- [5] Kisselev, A., 2009. Short overview on the PARAMETER program at LUTCH. Proceedings of 15th Int. QUENCH Workshop, Karlsruhe, Germany. November. ISBN 978-3-923704-71-2.
- [6] Ch. Duriez, M. Steinbrueck, D. Ohai, T. Meleg, J. Birchley and T. Haste, Separate-effect tests on zirconium cladding degradation in air ingress situations. Nuclear Engineering and Design, 239, 2009, pp. 244–253.
- [7] A. Miassoedov, “LACOMEKO project within the 7th EU FWP large scale experiments on core degradation, melt retention and containment behaviour.” Proceedings of the 15th International QUENCH Workshop, Karlsruhe, November 3-5, 2009. CD-ROM, ISBN 978-3-923704-71-2.
- [8] J. Stuckert, Z. Hozer, J. Moch, C. Roessger, U. Stegmaier, M. Steinbrueck, “Experimental results of the QUENCH-16 bundle tests on air ingress, performed within the framework of the LACOMEKO project. 17th International QUENCH Workshop”, Karlsruhe, 22-24 November 2011. ISBN: 978-3-923704-77-4.
- [9] I. Nagy, Z. Hózer, “QUENCH test with slow oxidation in air”. 16th International QUENCH Workshop, Karlsruhe, 16-18 November 2010 ISBN: 978-3-923704-74-3
- [10] J. Birchley, L. Fernandez-Moguel, C. Bals, E. Beuzet, Z. Hozer, J Stuckert, “WP5.1: Conduct and analytical support to air ingress experiment QUENCH-16”. 5th European Review Meeting on Severe Accident Research (ERMSAR-2012), Cologne (Germany), March 21-23, 2012.
- [11] L. Siefken, Private communication to J. Birchley (March 2011).
- [12] R. O. Gauntt et al., Code Manuals – Version 1.8.6, USNRC NUREG/CR 6119 Rev. 3, SAND2005-5713, Sandia National Laboratories, September, 2005.

- [13] J. Birchley and L. Fernandez-Moguel, "Simulation of air oxidation during a reactor accident sequence: Part 1 – Phenomenology and model development", *Ann. Nucl. Energy*, 40, 2012, pp. 163-170.
- [14] L. Fernandez-Moguel and J. Birchley, "Simulation of air oxidation during a reactor accident sequence: Part 2 – Analysis of PARAMETER-SF4 air ingress experiment using RELAP/SCDAPSIM", *Ann. Nucl. Energy*, 40, 2012, pp. 141-152.
- [15] R.E. Pawel, J.V. Cathcart and R.A McKee, "The kinetics of oxidation of zircaloy-4 in steam at high temperatures", *J. of Electrochemical Society*, 126, 1979, pp. 1105-1111.
- [16] V. H. Urbanic and T. R.Heidrick, "High-temperature oxidation of zircaloy-2 and zircaloy-4 in steam", *J. Nuclear Materials.*, 75, 1978, pp. 251-261.
- [17] H. Uetsuka and P. Hofmann, "Reaction kinetics of zircaloy-4 in a 25% O<sub>2</sub> / 75% Ar gas mixture under isothermal conditions", *Forschungszentrum Karlsruhe Report KFK 3917*, May 1985.
- [18] J. Birchley, T. Haste, C. Homann and W. Hering, "Pre-test analytical support for experiments QUENCH-10, -11 and -12", Paper 812, *Proc. Conf. Nuclear Energy in New Europe 2006*, Portoroz, Slovenia.
- [19] J. Birchley and J. Stuckert, "Analysis of QUENCH-ACM experiments using SCDAP/RELAP5", Paper 10289, *Proceedings of ICAPP '10*, San Diego, USA, June 13-17, 2010.
- [20] W. Hering, Ch. Homann, J. S. Lamy, A. Miassoedov, G. Schanz, L. Sepold, M. Steinbrueck, "Comparison and interpretation report of the OECD International Standard Problem No. 45 exercise (QUENCH-06), OECD/NEA/CSNI/R(2002)2, *Wissenschaftliche Berichte*, FZKA-6722, November 2002.
- [21] M. Steinbrück, U. Gerhards, M. Große, H. Leiste, S. Prestel, U. Stegmaier. "Recent results of KIT separate-effects tests on oxidation of zirconium alloy cladding". 17th International QUENCH Workshop, Karlsruhe, 22-24 November 2011. ISBN: 978-3-923704-77-4.
- [22] M. Steinbrück, M. Jung. "New results on the mechanism of Zircaloy-4 oxidation in air. 16th International QUENCH Workshop", Karlsruhe, 16-18 November 2010, ISBN: 978-3-923704-74-3